ARTICLE NO. 80-4079

J80-184

60002
60003
60008

Model for Double-Base Propellant Combustion

M. W. Beckstead*
Brigham Young University, Provo, Utah

The Beckstead-Derr-Price (BDP) monopropellant model that was originally developed as a limiting case for composite propellants has been modified and applied to double-base propellants. The work was performed with the intent of applying the model to modern double-base systems of interest in rocket propulsion. Therefore, the model has been developed to predict burn rate as a function of pressure, initial temperature, and the double-base binder energy. The model has been compared to a set of experimental data covering a wide range of pressures, initial temperatures, and binder energy with excellent agreement. A comparison with 81 test conditions resulted in 96% of the predictions within ± 10% of the data and a maximum error of 12%. All of the calculated rates, sensitivities, and combustion parameters using the double-base model appear to be consistent with available experimental data. The quantitative predictions of the model varying pressure, initial temperature, and binder energy are considered a significant advance in the state of the art.

Nomenclature

A = Arrhenius frequency factor
c_P = average mean heat capacity for the solid and gases
E = activation energy
Hex = heat of explosion
k = rate constant
M = mass flux
n = pressure exponent of burn rate
P = pressure
Q = heat release associated with combustion steps
Q_L = condensed-phase heat of gasification
r = linear burning rate
R = gas constant
T = temperature
T_f = adiabatic flame temperature of the dark zone
T_0 = initial temperature of the propellant
x^* = flame standoff distance
δ = reaction order
ξ^* = nondimensional flame standoff distance
σ_p = temperature sensitivity, $d \ell nr/dT_0$
ρ = density
λ = thermal conductivity of gases

Subscripts

f = flame condition
ref = reference condition
s = burning surface

Introduction

DOUBLE-base propellants have been used widely in both rockets and guns for many years. Relatively successful models describing the combustion of double-base propellants were developed in the late 1940's and early 1950's by various authors.[1-6] The models typically follow the temperature profile from the initial temperature through the final combustion products. Figure 1 shows the generally accepted structure of a double-base propellant flame. Spaulding[7] reviewed the state of modeling in 1960, and the most recent modeling work has been performed by Kubota,[8,9] Suh,[10,11] and Ibiricu.[12,13] Suh and Ibiricu were modeling a specific gun propellant while Kubota's work was directed at catalyzed double-base propellants. Most of these models have compared burn rate vs pressure for a single propellant. Very few have examined the influence of initial temperature, and none have explored the effects of heat of explosion (i.e., propellant composition).

The current modeling work represents a limiting condition for a more comprehensive model for both composite and composite-modified double-base (CMDB) propellants. The model presented here is essentially the Beckstead-Derr-Price (BDP) monopropellant model[14] applied to a double-base propellant. The overall model is being developed with the intent of applying it to modern CMDB and crosslinked double-base (XLDB) propellant systems. Therefore, as a limiting condition, it has been compared to a series of unfilled double-base binders typical of what could form the backbone binder of a modern double-base propellant. Because of this objective, the binder energy Hex is considered as a primary variable.

This paper includes a discussion of the approach used to calculate dark zone temperatures as a function of both pressure and binder energy. Then, the equations representing the model are presented. Finally, the model is compared with experimental data at varying pressure, initial temperature, and binder energy.

Flame Temperature Predictions

Adaptation of the BDP approach to a double-base system requires an a priori determination of the double-base flame temperatures as input to the model. The final flame is over 1000 μ from the surface[8,15] for pressures of 100 atm and less, and is too far away to transfer any significant amount of heat to the surface. From Fig. 1, the dark zone flame is closest to the propellant surface and dominates the combustion process for relatively low pressures.[4-8] Previous work in this area was done by Heller and Gordon[15] and Sotter,[16] but provides a very inadequate data base for a comprehensive approach. Heller and Gordon sampled combustion gases in the dark zone and then used infrared and mass spectrometer techniques for determining gas composition, but their testing was only done at pressures below 34 atm and for three very similar propellants. A thermocouple was used to measure temperatures. Sotter did an excellent theoretical study on the kinetics of postulated species, but he only made calculations at one pressure (68 atm) and for a single propellant composition. His results are in reasonable agreement with experimental data.

Received Oct. 1, 1979; revision received Jan. 8, 1980.

Index categories: Combustion and Combustor Designs; Combustion Stability; Ignition and Detonation; Fuels and Propellants, Properties of.

*Associate Professor, Dept. of Chemical Engineering. Associate Fellow AIAA.

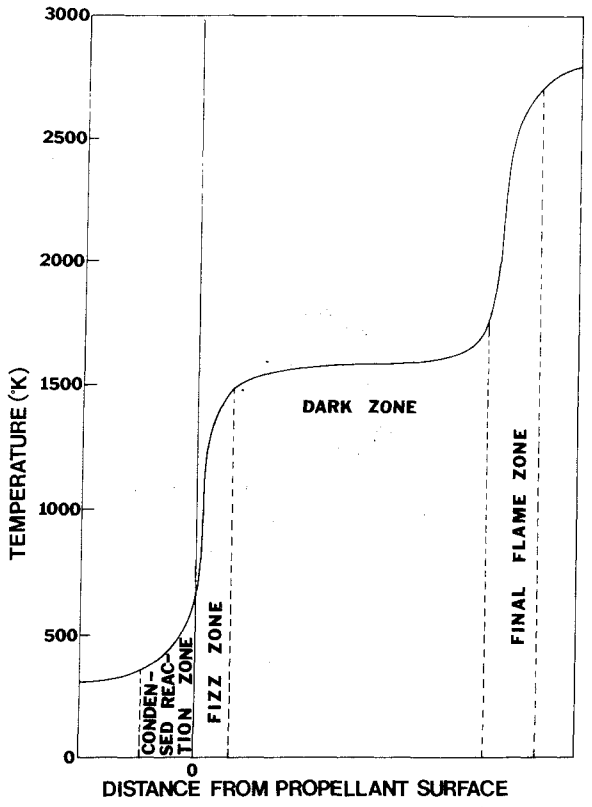

Fig. 1 Structure of double-base propellant combustion.

As part of the current study, it was desirous to vary pressure, initial temperature, and propellant energy; therefore, it was necessary to develop a technique to calculate the dark zone temperature a priori due to the lack of experimental data or previous calculations. A complex kinetic study such as Sotter's was beyond the scope of the current project; therefore, a simpler approach was developed.[17] A standard thermochemical computer program was used to predict the temperatures, but nitrogen species were not allowed to be reduced to N_2 nor N_2O to simulate the dark zone characteristics. This was justified on the basis that very little N_2 is observed in the dark zone.[15,16] Initial attempts were made to restrict N_2 in the product species. However, it was found that most of the nitrogen in the system was calculated to be reduced to N_2O, yielding temperatures of ~2000 K and very little NO. Experimental data[15] do not detect N_2O; therefore, N_2O was also restricted from the product species. Using this approach, the equilibrium gas composition shown in Table 1 was calculated. The calculations are compared to both Heller and Gordon's data and to Sotter's calculations. Heller and Gordon did not measure H_2O, but estimated an H_2O content of 30%; their data are proportioned accordingly. The calculated results are in very reasonable agreement. Considering that N_2 was excluded from the products, more NO than actual would be anticipated, which would also reduce the calculated amount of H_2O. This trend is consistent with the calculated results. The calculations are also shown in Fig. 2 as a function of binder *Hex*.

The calculated temperature is much lower than the experimental data. Again, if some of the NO were reduced to N_2, the temperature would be increased, thus explaining the lower calculated temperature. To match Heller and Gordon's data and Sotter's calculations, the calculated temperature at 68 atm and 1000 *Hex* was corrected by adding 500 K to the calculation. Additional data at different pressures, temperatures, or binder *Hex* were not found in the literature. Thus, there is no way to predict accurately the dark zone

Table 1 Calculated fizz zone characteristics

	Composition (mole %)		
	Heller & Gordon experimental data	Sotter's kinetic calculations	Equilibrium calculations
Species			
CO	28	30	30
NO	21	20	29
H_2	7	5	17
CO_2	8	10	12
H_2O	30	27	11
CH_4	1	0	1
N_2	4	8	—
Temperature (K)	1700[a]	1600	1100
Conditions			
Binder *Hex* (cal/g)	1315	1000	1000
Pressure (atm)	68	68	68

[a] Extrapolated from data below 20 atm.

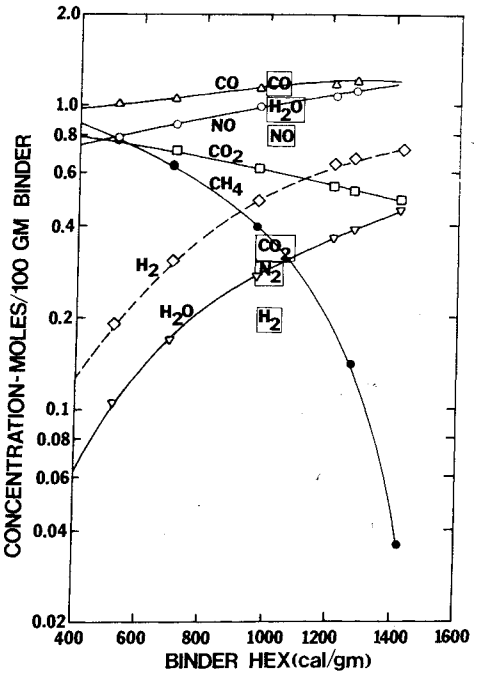

Fig. 2 Calculated fizz zone concentration at 68 atm as a function of binder heat of explosion (Sotter's calculations are shown as boxes at 1000 *Hex*).

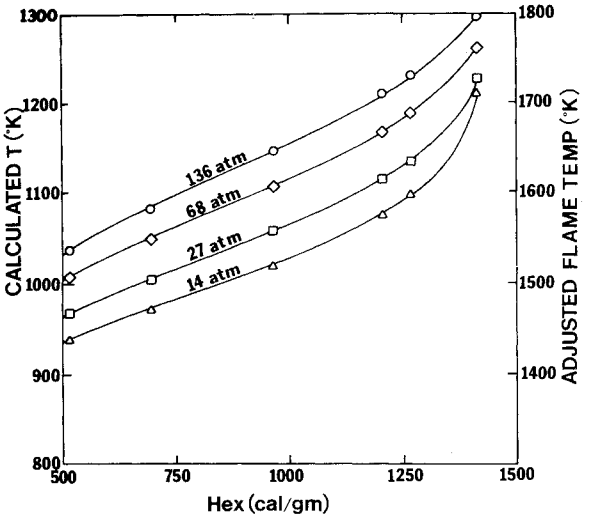

Fig. 3 Calculated fizz zone flame temperature using Howard's method.

temperatures for the wide range of conditions desired. In lieu of having accurate data available, the 500 K correction was made to all of the calculations; hopefully, additional data or other predictive techniques will be developed at some time in the future. Although the temperature calculation is not precise, using the one available datum point for making corrections does allow the a priori calculation of an equilibrium temperature as a function of pressure and binder *Hex*. The calculations (see Fig. 3) show the temperature increasing with increasing pressure and increasing binder *Hex*, which are the anticipated trends. These adjusted temperatures have been programmed into the computer program and are used for all double-base calculations.

Theoretical Model

Within the framework of the BDP model, double-base combustion can be represented by applying the BDP monopropellant model[14] to an unfilled binder. The model reduces to essentially three equations: one describing the surface kinetics; one resulting from an energy balance at the burning surface; and one related to the gas-phase kinetics.

The surface regression is described as a one-step, zero-order Arrhenius function

$$M_s = A_s e^{-E_s/RT_s} \tag{1}$$

The surface temperature is assumed to be uniform over the burning surface and is derived from an energy balance at the surface. It can be expressed as

$$T_s = T_0 - \frac{Q_L}{c_p} + \frac{Q_f}{c_p} e^{-\xi^*} \tag{2}$$

where T_0 corresponds to the initial energy in the system, the term involving Q_L corresponds to the condensed-phase energy released at the burning surface, and the final term represents the energy transported from the flame back to the surface. The heat released in the flame is calculated from an overall energy balance

$$Q_f = c_p(T_f - T_0) - Q_L \tag{3}$$

where T_f is the adiabatic flame temperature. Equation (3) requires the flame temperature calculation discussed in the previous section.

For a premixed laminar flame, the nondimensional flame-standoff distance can be represented by

$$\xi^* = c_p M_s x^*/\lambda = c_p M_s/(\lambda k P^\delta) \tag{4}$$

where the gas-phase rate constant k is

$$k = A_f e^{-E_f/RT_f} \tag{5}$$

Because the rate appears in both Eqs. (1) and (4), an iterative solution is required in the calculation. The numerical iteration routine in the computer program is based on the controlling mechanism being the gas-phase flame. Equation (4) is solved for the flame-standoff distance; then, Eq. (2) is solved for surface temperature; and finally, Eq. (1) is solved for the rate. Where condensed-phase effects dominate the rate, i.e., at low pressures, this iteration approach becomes divergent, i.e., $\xi^* \to \infty$. Therefore, a reverse iteration approach was developed and is used at low pressure, and then must be averaged with the conventional approach as pressure is incremented.

One advantage of the BDP model is its simplicity. The equations are sufficiently tractable that they can be differentiated to obtain closed-form solutions for both pressure and temperature dependence.

The pressure exponent is

$$n = \left[\delta + \left(\frac{E_f}{RT_f} + \frac{c_p T_f}{Q_f \xi^*}\right)\frac{d\ln T_f}{d\ln P}\right] \Big/ \left[2 + \frac{RT_s}{E_s}\frac{c_p T_s}{Q_f \xi^* e^{-\xi^*}}\right] \tag{6}$$

An order-of-magnitude evaluation of the various parameters shows that the pressure exponent will be a little less than half of the gas-phase reaction order, which is the normally expected value.

The temperature sensitivity is

$$\sigma_p = \left[\frac{c_p}{Q_f \xi^* e^{-\xi^*}} + \frac{E_f}{RT_f}\frac{d\ln T_f}{dT_0}\right] \Big/ \left[2 + \frac{RT_s}{E_s}\frac{c_p T_s}{Q_f \xi^* e^{-\xi^*}}\right] \tag{7}$$

In this form, it can be seen that the denominators are identical for both n and σ_p. Based on this equation, σ_p can be evaluated in terms of flame temperature, activation energy, etc.

Another convenience of the BDP approach is the ability to evaluate limiting conditions. Pokhil[18] suggests testing at elevated temperature and vacuum to determine condensed-phase activity. For these conditions, the above equations reduce to

$$M_s = A_s e^{-E_s/RT_s} = M_{s_{\text{ref}}} \exp\left[-\frac{E_s}{R}\left(\frac{1}{T_s} - \frac{1}{T_{s\text{ref}}}\right)\right] \tag{8}$$

$$T_s = T_0 - (Q_L/c_p) + \text{negligible heat from flame} \tag{9}$$

Thus, if the surface temperature can be measured for these conditions, the Q_L term (condensed-phase heat release) can be calculated directly from Eq. (9) as

$$Q_L = -c_p(T_s - T_0)_{\text{vacuum}} \tag{10}$$

If burning rate is also measured along with surface temperature, then either the activation energy E_s or prefactor A can be determined. If burn rate and surface temperature are determined varying the initial temperature, all three parameters can be determined.

Using this approach, Pokhil[18] and Suh[10] have estimated the magnitude of the condensed-phase reaction for double-base propellants based on experiments. Their data indicate a condensed heat release of ~50 cal/g (exothermic). Kubota's experiments[8] indicate a value of ~70-90 cal/g. Within the context of the model, the magnitude of Q_L makes little difference in the predicted results above 30 atm. However, for accurate predictions at low pressures, a precise evaluation of the condensed-phase effects is necessary. Furthermore, for application to a variety of modern propellants, the effects must be known fairly accurately as a function of binder *Hex*.

The Miller-Foster[19] data discussed in the next section show a very pronounced effect of condensed-phase reactions at low pressure as the pressure exponent approaches zero. Based on Eqs. (8-10), their low-pressure data can be utilized to evaluate consistent values of Q_L, E_s, and A_s (or $T_{s\text{ref}}$) within the model. This was done, and it was found that Q_L must be a weak function of binder *Hex* with a nominal value of -75 cal/g (exothermic). Based on the low-pressure data, the optimized equation for Q_L is

$$Q_L \cong -65.7 - 0.013\,Hex$$

This results in $Q_L = -81$ cal/g for a *Hex* of 1200 cal/g and $Q_L = -73$ cal/g for a *Hex* of 600 cal/g, which is in reasonable agreement with experimental determinations for other propellants.[8,10,18] The dependence of Q_L on the binder energy is not surprising.

Comparison of Model and Experimental Data

The model was compared to available experimental data. The burn rate of double-base propellants is strongly

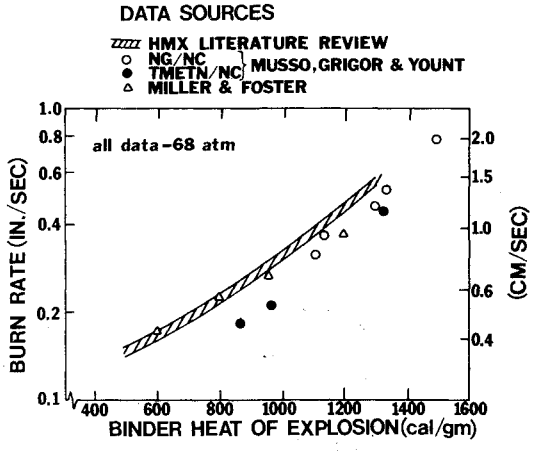

Fig. 4 Double-base propellant burn rate as a function of propellant heat of explosion.

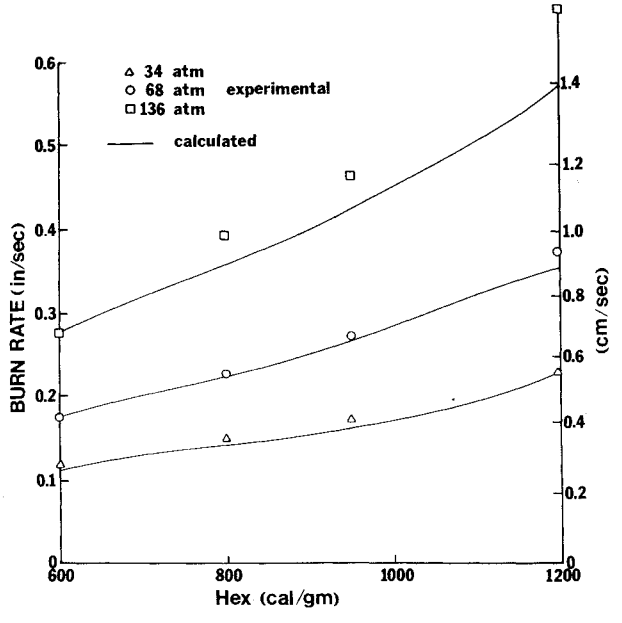

Fig. 5 Comparison of calculated and experimental rates as a function of binder *Hex* for varying pressure.

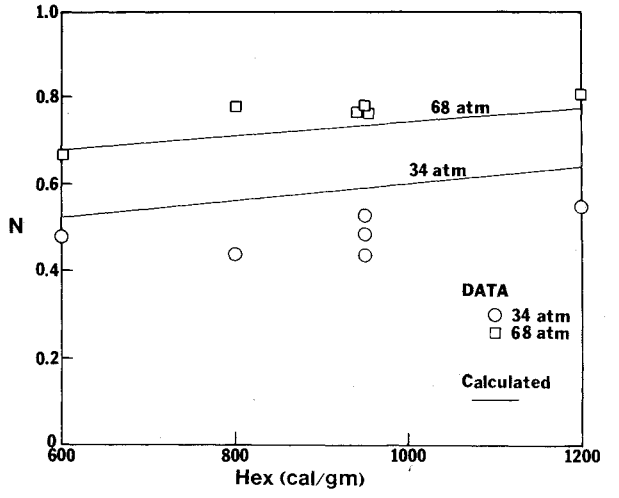

Fig. 6 Comparison of calculated and experimental pressure exponents as a function of binder *Hex* for varying pressure.

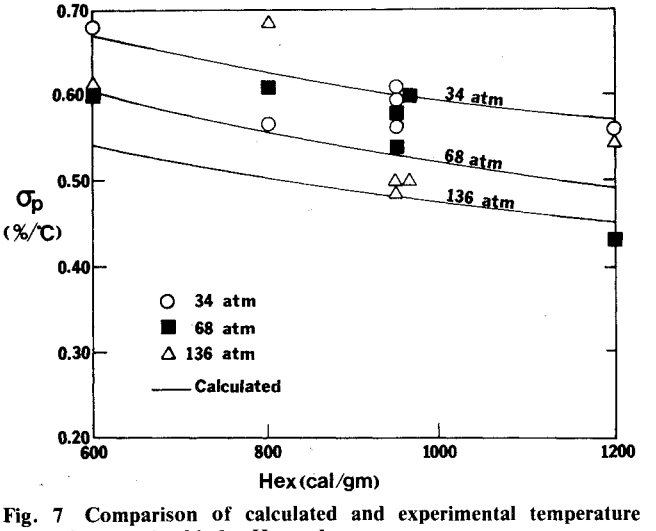

Fig. 7 Comparison of calculated and experimental temperature sensitivities varying binder *Hex* and pressure.

dependent on the binder *Hex*; therefore, data were sought where *Hex* had been varied. Three sources were found,[19-21] and the data are plotted in Fig. 4. Careful examination of the combined data shows that the burn rate correlates very well with binder *Hex* for the nitrocellulose/nitroglycerin (NG/NC) systems. However, the trimethylol ethane trinitrate (TMETN) propellants with equivalent binder *Hex* have lower rates. Therefore, if the model is to be used for energetic binders other than NG/NC systems, some compensation will have to to be made to the input parameters, probably in the dark zone prefactor term A_f. The data of Miller and Foster are the most complete. Propellant *Hex* values range from 600 to 1200 cal/g; pressures range from 3 to 200 atm (50 to 3000 psi); and initial temperature varies from 260 to 340 K (10 to 155°F). Therefore, their set of data was selected for the comparison that follows.

In attempting to match the data, one observation became obvious very quickly. Double-base propellants have a pressure exponent of ~0.6-0.8 at 70 atm, apparently increasing slightly with binder energy. Examining Eq. (6) for the pressure exponent and recognizing from Fig. 3 that $d\ell nT/d\ell nP$ is ~0.05, it is apparent that the dark zone reaction must be approximately first-order. Also, to match the rate vs *Hex* dependence at high pressure, a dark zone activation energy of ~50 kcal/mole must be assumed. This activation energy plus the pressure-dependent flame temperatures and a first-order reaction results in the desired pressure exponent as a function of binder *Hex*.

Calculations were made with the model to simulate the Miller-Foster data over the entire range of pressure, temperature, and binder *Hex*. This included 81 datum points. Model parameters that are not well specified in the literature were varied to determine an optimized statistical fit between the model and the data. The model parameters that were varied include: E_f, the gas-phase activation energy; E_s, the surface reaction activation energy; and T_{sref}, the reference surface temperature. The optimized statistical fit of the data is summarized in Table 2, comparing the predicted rates to the experimental rates at all 81 test conditions. The results are excellent. All the predictions fall within ±12% of the data, and 96% fall within ±10%.

Figure 5 shows a plot of rate vs *Hex* at 34, 68, and 136 atm (500, 1000, and 2000 psi), comparing the model predictions to the data. The only significant deviation occurs at 136 atm where the predictions become increasingly low with *Hex* (up to an 11% error). Figure 6 shows the predicted exponent compared to experimental data. The agreement is excellent although the predicted exponents are slightly higher than experiment at 34 atm.

Calculations have also been made varying the initial temperature of the propellant. The calculated temperature

Table 2 Comparison of predicted and experimental rates of double-base propellants

Pressure (psi)	Initial temp (K)	Predicted rate (in./s)	Experimental rate (in./s)	% Error	Binder *Hex* (cal/g)
115	298	0.065	0.067	−3.0	600
315	"	0.089	0.092	−3.6	"
515	"	0.117	0.116	1.2	"
715	"	0.143	0.138	3.7	"
1015	"	0.182	0.170	7.2	"
2015	"	0.282	0.280	0.9	"
3015	"	0.393	0.377	4.2	"
65	"	0.075	0.076	−1.5	800
115	"	0.075	0.081	−7.8	"
315	"	0.109	0.118	−7.8	"
515	"	0.147	0.144	1.8	"
715	"	0.180	0.172	4.5	"
1015	"	0.230	0.223	3.3	"
2015	"	0.366	0.390	−6.3	"
3015	"	0.511	0.521	−2.0	"
65	"	0.083	0.082	0.7	950
115	"	"	0.092	−8.8	"
"	"	"	0.095	−12.2	"
"	"	"	0.090	−7.3	"
315	"	0.126	0.135	−6.5	"
"	"	"	0.137	−7.9	"
"	"	"	0.134	−5.8	"
515	"	0.171	0.171	−0.2	"
"	"	"	0.171	−0.2	"
"	"	"	0.170	0.4	"
715	"	0.209	0.204	2.6	"
"	"	"	0.199	5.2	"
"	"	"	0.210	−0.3	"
1015	"	0.271	0.265	2.2	"
"	"	"	0.258	5.0	"
"	"	"	0.269	0.7	"
2015	"	0.434	0.455	−4.6	"
"	"	"	0.443	−2.0	"
"	"	"	0.464	−6.5	"
3015	"	0.611	0.582	5.0	"
"	"	"	0.570	7.2	"
"	"	"	0.594	2.9	"
65	"	0.098	0.099	−0.9	1200
115	"	0.104	0.105	−1.0	"
315	"	0.168	0.175	−4.3	"
515	"	0.227	0.222	2.3	"
715	"	0.280	0.280	−0.1	"
1015	"	0.365	0.370	−1.2	"
2015	"	0.586	0.658	−11.0	"
3015	"	0.829	0.896	−7.5	"
515	341	0.164	0.155	5.7	600
1015	"	0.237	0.216	9.6	"
2015	"	0.360	0.352	2.4	"
515	"	0.197	0.183	7.7	800
1015	"	0.294	0.283	3.7	"
2015	"	0.456	0.496	−8.2	"
515	"	0.226	0.218	3.6	950
"	"	"	0.218	3.6	"
"	"	"	0.222	1.8	"
1015	"	0.341	0.332	2.7	"
"	"	"	0.331	3.0	"
"	"	"	0.328	4.0	"
2015	"	0.534	0.542	−1.5	"
"	"	"	0.543	−1.6	"
"	"	"	0.545	−2.0	"
515	"	0.292	0.283	3.2	1200
1015	"	0.452	0.443	2.1	"
2015	"	0.708	0.804	−11.9	"
515	261	0.092	0.090	1.9	600
1015	"	0.147	0.134	9.7	"
2015	"	0.232	0.216	7.4	"
515	"	0.116	0.116	0.3	800
1015	"	0.189	0.174	8.4	"
2015	"	0.302	0.288	4.7	"
515	"	0.137	0.138	−0.7	950
"	"	"	0.135	1.5	"
"	"	"	0.136	0.8	"
1015	"	0.223	0.208	7.2	"
"	"	"	0.204	9.3	"
"	"	"	0.207	7.7	"
2015	"	0.365	0.364	0.2	"
"	"	"	0.363	0.5	"
"	"	"	0.370	−1.4	"
515	"	0.186	0.180	3.2	1200
1015	"	0.304	0.314	−3.3	"
2015	"	0.498	0.517	−3.6	"

Square of the correlation coefficient for the data is 0.986.
Standard error of estimate is 0.0022.
Number of data points is 81.
78 points are within 10%; 81 points are within 20%.
Maximum deviations are +9.7%, and −12.2%

Parameter values

Surface activation energy (EF) = 10,000 cal/g
Flame activation energy (EDB) = 54,000 cal/g
Reference surface temp (TSREF) = 600 K
Binder density (RHOF) = 1.55 g/cc
Binder specific heat (CSUBPB) = 0.35 cal/g K
Flame reaction order (XNDB) = 1.0

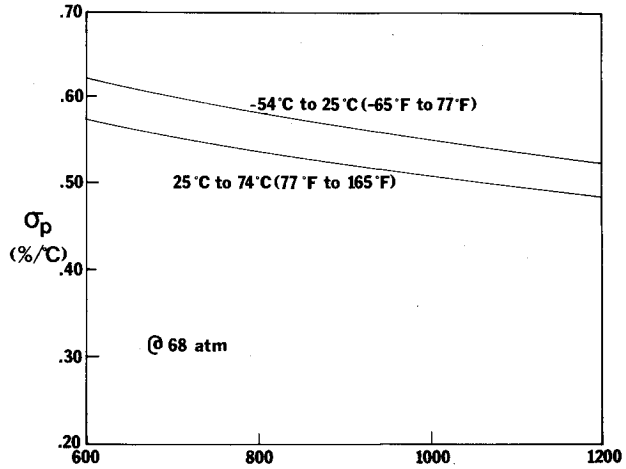

Fig. 8 Predicted dependence of temperature sensitivity on initial temperature.

sensitivity σ_p is plotted vs the binder *Hex* in Fig. 7. The calculations show σ_p decreasing with increasing *Hex* and with increasing pressure. Additional calculations show that σ_p increases with increasing gas-phase activation energy and with increasing condensed-phase heat release. The magnitude of the numbers as well as the trends appears to be very consistent with the data, recognizing that the data scatter obscures the data trends somewhat. It must be recognized that σ_p data are normally good to between ~20 and 50% depending on the number and quality of datum points obtained. Figure 8 shows the dependence of σ_p on initial temperature with values calculated from 219 to 298 K (−65°F to 77°F) and from 298 to 347°K (77°F to 165°F). The temperature sensitivity increases slightly with increasing temperature.

Measured values of the surface temperature for double-base propellants vary between 250 and 400°C.[8,11,22] No data were found where the dependence on binder *Hex* was systematically evaluated, but surface temperatures have generally been observed to increase with pressure. Figure 9 shows the predicted surface temperatures which increase with

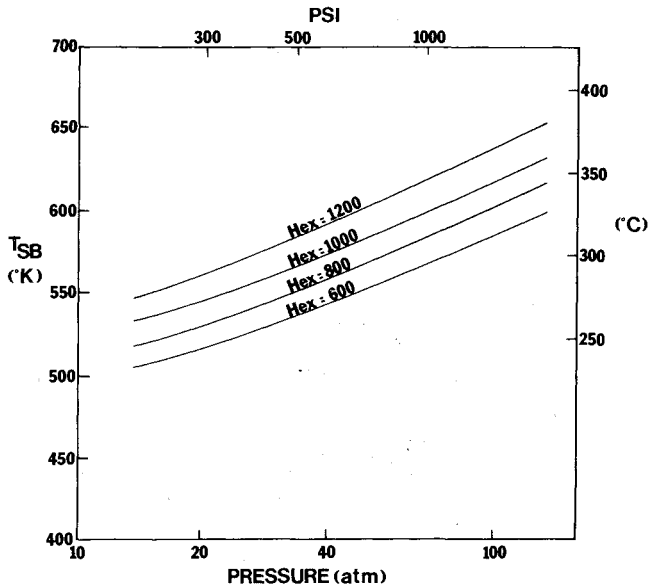

Fig. 9 Predicted surface temperature for varying binder *Hex* and pressure.

increasing pressure and increasing *Hex* from 230 to 380°C. The magnitude of the values is in agreement with experimental values of T_s. Both trends appear to be consistent. Binders with increasing energy have increasing rates and, therefore, should have higher surface temperatures. Systematic experimental data on the subject would be very worthwhile to verify these predicted trends.

Conclusions

All of the calculated trends with the double-base model appear to be consistent. The direct comparison with available experimental data shows greater quantitative agreement than ever before published for a double-base model. Previous models have only compared rates as a function of pressure and usually for only one or two propellants. No previous model has predicted the effect of binder energy or initial temperature. Therefore, the quantitative predictions of the current model considering pressure, initial temperature, and binder energy must be considered as a significant advance in the state of the art.

Acknowledgments

This work was sponsored by AFRPL on Contracts F04611-78-C-0005 and F04611-76-C-0019 to Hercules, Inc., and the BYU work was sponsored by subcontracts from Hercules. The author would also like to recognize the many fruitful discussions held with K. P. McCarty of Hercules, Inc.

References

[1] Boys, S. F. and Corner, J., "The Structure of the Reaction Zone in a Flame," *Proceedings of the Royal Society*, London, Vol. A197, No. 1048, 1949, pp. 90-106.

[2] Corner, J., "The Effects of Diffusion of the Main Rectants on Flame Speeds in Gases," *Proceedings of the Royal Society*, London, Vol. A198, No. 1054, 1949, pp. 388-405.

[3] Corner, J., *Theory of the Interior Ballistics of Guns*, Wiley, New York, 1950.

[4] Rice, O. K. and Ginell, R., "Theory of Burning of Double-Base Rocket Powders," *Journal of Physics and Colloid Chemistry*, Vol. 54, No. 6, 1950, pp. 885-917.

[5] Parr, R. G. and Crawford, B. L., "A Physical Theory of Burning of Double-Base Rocket Propellants," *Journal of Physics and Colloid Chemistry*, Vol. 54, No. 6, 1950, pp. 929-954.

[6] Adams, G. K. and Wiseman, L. A., "The Combustion of Double-Base Propellants," *Selected Combustion Problems*, Butterworth Scientific Publications, London, England, 1954, pp. 277-288.

[7] Spalding, D. B., "The Theory of Burning of Solid and Liquid Propellants," *Combustion and Flame*, Vol. 4, No. 1, March 1960, pp. 59-76.

[8] Kubota, N., et al., "The Mechanism of Super-Rate Burning of Catalyzed Double-Base Propellants," *15th Symposium (International) on Combustion*, The Combustion Institute, Pittsburgh, Penn., 1974, pp. 529-537; also, *Aerospace and Mechanical Sciences Report No. 1087*, Princeton University, Princeton, N.J., March 1973.

[9] Kubota, N. and Masamoto, T., "Flame Structures and Burning Rate Characteristics of CMDB Propellants," *16th Symposium (International) on Combustion*, The Combustion Institute, Pittsburgh, Penn., 1977, pp. 1201-1209.

[10] Kirby, C. E. and Suh, N. P., "An Experimental Method for Determining the Condensed-Phase Heat of Reaction of Double-Base Propellants," *AIAA Journal*, Vol. 9, April 1971, pp. 754-756.

[11] Thompson, C. L. and Suh, N. P., "Gas-Phase Reactions Near the Solid-Gas Interface of a Deflagrating Double-Base Propellant Strand," *AIAA Journal*, Vol. 9, Jan. 1971, pp. 154-159.

[12] Ibiricu, M. M. and Williams, F. A., "Mechanisms for the Steady Deflagration of Double-Base Propellants," *12th JANNAF Combustion Meeting*, Johns Hopkins Univ., Laurel, Md., Vol. II, CPIA No. 273, Dec. 1975, pp. 283-299.

[13] Ibiricu, M. M. and Williams, F. A., "Steady Deflagration of Double-Base Propellants at Elevated Pressures," *13th JANNAF bustion Meeting*, John Hopkins Univ., Laurel, Md., Vol. 1, CPIA No. 281, Dec. 1976, pp. 253-257.

[14] Beckstead, M. W., Derr, R. L., and Price, C. F., "The Combustion of Solid Monopropellants and Composite Propellants," *13th Symposium (International) on Combustion*, The Combustion Institute, Pittsburgh, Penn., 1971, pp. 1047-1056.

[15] Heller, C. A. and Gordon, A. S., "Structure of the Gas-Phase Combustion Region of a Solid Double-Base Propellant," *Journal of Physical Chemistry*, Vol. 59, 1955, pp. 773-777.

[16] Sotter, J. C., "Chemical Kinetics of the Cordit Explosion Zone," *10th Symposium on Combustion*, The Combustion Institute, Pittsburgh, Penn., 1965, pp. 1401-1411.

[17] Howard, W. S., unpublished calculations, Hercules Inc., Dec. 1976; see also McCarty, K. P., and Beckstead, M. W., "HMX Propellant Combustion Studies," Hercules, Inc., Magna, Utah, AFRPL-TR-78-73, Nov. 1978.

[18] Pokhil, P. F., Logacheo, V. S., and Mal'tsev, M. W., "The Mechanism of Metal Particle Combustion," *Combustion Explosion and Shock Waves*, Vol. 6, No. 3, 1970, p. 356.

[19] Miller, R. R. and Foster, R. L., personal communication, Hercules Inc., ABL, Cumberland, Md., Aug. 1978 (data generated on Contract F04611-78-C-0005).

[20] McCarty, K. P., Beckstead, M. W., and Simmons, R. L., "HMX Propellant Combustion Studies," Hercules Inc., Magna, Utah, AFRPL-TR-76-59, Dec. 1976.

[21] Musso, R. C., Grigor, R., and Yount, R. A., "Combustion Mechanism of Low-Burning Rate Propellant," Hercules Inc., ABL, Cumberland, Md., AFRPL-TR-69-130, May 1969.

[22] Klein, R., Mentser, M., von Elbe, G., and Lewis, B., "Determination of the Thermal Structures of a Combustion Wave by Fine Thermocouples," *Journal of Physics and Colloid Chemistry.*, Vol. 54, No. 6, 1950, pp. 877-884.